

  
**MITSUBISHI HEAVY INDUSTRIES, LTD.**  
16-5, KONAN 2-CHOME, MINATO-KU  
TOKYO, JAPAN

February 4, 2010

Document Control Desk  
U.S. Nuclear Regulatory Commission  
Washington, DC 20555-0001

Attention: Mr. Jeffery A. Ciocco

Docket No. 52-021  
MHI Ref: UAP-HF-10033

**Subject:** MHI's Responses to US-APWR DCD RAI No. 490-3732

**Reference:** 1) "Request for Additional Information No. 490-3732 Revision 0, SRP Section: 03.08.01 - Concrete Containment," dated 11/23/2009.

With this letter, Mitsubishi Heavy Industries, Ltd. ("MHI") transmits to the U.S. Nuclear Regulatory Commission ("NRC") a document entitled "Responses to Request for Additional Information No. 490-3732, Revision 0."

Enclosed are the responses to 9 RAIs contained within Reference 1. This transmittal completes the response to this RAI.

Please contact Dr. C. Keith Paulson, Senior Technical Manager, Mitsubishi Nuclear Energy Systems, Inc. if the NRC has questions concerning any aspect of this submittal. His contact information is provided below.

Sincerely,

*Y. Ogata*

Yoshiki Ogata,  
General Manager- APWR Promoting Department  
Mitsubishi Heavy Industries, LTD.

Enclosure:

1. Responses to Request for Additional Information No. 490-3732, Revision 0

CC: J. A. Ciocco  
C. K. Paulson

Contact Information

C. Keith Paulson, Senior Technical Manager  
Mitsubishi Nuclear Energy Systems, Inc.  
300 Oxford Drive, Suite 301  
Monroeville, PA 15146  
E-mail: ck\_paulson@mnes-us.com  
Telephone: (412) 373-6466

*DOB1  
NRC*

Docket No. 52-021  
MHI Ref: UAP-HF-10033

Enclosure 1

UAP-HF-10033  
Docket No. 52-021

Responses to Request for Additional Information No. 490-3732,  
Revision 0

February, 2010

---

---

**RESPONSE TO REQUEST FOR ADDITIONAL INFORMATION**

---

---

2/4/2010

**US-APWR Design Certification  
Mitsubishi Heavy Industries  
Docket No. 52-021**

**RAI NO.:** NO. 490-3732 REVISION 0  
**SRP SECTION:** 03.08.01 - Concrete Containment  
**APPLICATION SECTION:** 3.8.1  
**DATE OF RAI ISSUE:** 11/23/2009

---

**QUESTION NO. RAI 03.08.01-2:**

NOTE: This question and all other questions in this Request for Additional Information (RAI) were based on Revision 1 of the Design Control Document (DCD). These questions were written prior to the receipt of DCD Revision 2 on 10/28/2009. If the response to a question can be found in Revision 2, the applicant needs to identify where and how the response is provided.

In its response to Question 3.8.1-1 (of RAI 223-1996 hereinafter unless indicated otherwise, dated 4/14/2009, MHI Ref: UAP-HF-09161, ML091060749), Mitsubishi Heavy Industries (MHI) points out that it is similar to Question 06.02.05-19 of RAI 62 dated 10/01/2008. MHI's position is that the structural integrity of the prestressed concrete pressure vessel (PCCV) should be evaluated with different criteria than that contained in RG 1.136 for severe accident cases. (It should be noted that this position is counter to the intent of RG 1.136 in which loadings to be considered include all types of accidental loads [specifically loss of coolant accident (LOCA), hydrogen burn, etc.]). Previously, in its evaluation of MHI's response to Question 06.02.05-19, the NRC staff's conclusion was that the response was unacceptable. The staff finds that the same conclusion applies in this current review of MHI's response to Question 3.8.1-1, namely, MHI's position as stated in the response is not acceptable because Regulatory Position 5 in RG 1.136 makes it clear that the applicant is to evaluate the containment structure for several severe accident loads, including loads associated with LOCA accidents and the effects of a hydrogen burn following a 100% fuel clad metal-water reaction. The staff subsequently issued follow-up Question 06.02.05-34 of RAI 270-1898. The following is the open item for this issue:

"Open Item 6.2.5-13: The staff requested, in RAI 6.2.5-19 (RAI 62) that the applicant clarify whether the load associated with dead load plus 45 psig, would result in higher containment loadings than would result from the loads associated with the releases of hydrogen generated from 100% metal-water reaction of the fuel cladding and accompanied by uncontrolled hydrogen burning.

The applicant provided the following response:

"MHI agrees that the NRC's concern is true, that the load associated with the release of hydrogen generated from 100% cladding-water reaction exceeds the one associated with dead load plus 45 psig. As for the MHI's understanding, it is necessary to separately consider the design-basis accident and severe accident for this issue. The discussion

provided in Section 3.8.1.3.2.2 of the DCD is based on the design-basis accident, thus 100% cladding reaction is not taken into account. The postulated condition with 100% cladding reaction is obviously significantly beyond the design-basis. The conclusion in Section 3.8.1.3.2.2 is therefore good only for the evaluation on the design-basis accidents. The USAPWR PCCV is designed based on a [Design Basis Accident] DBA pressure Pa of 68 psig and a corresponding design test pressure of  $1.15 \times Pa$ , hence the minimum design condition of D+45 psig is satisfied under the postulated conditions of DBA. On the other hand, Section 19.2 of the DCD describes the severe accident analyses, including the pressure load associated with the hydrogen released from 100% cladding-water reaction. Please refer to the technical report "US-APWR Probabilistic Risk Assessment" (MUAP-07030) Chapter 15 Separate Effect Analysis, in which detailed discussions on severe accident evaluations are provided. Section 15.3 of this report describes the discussion on the hydrogen generation and control, and the evaluations of the containment integrity under the hydrogen burning condition, including local burn and global burn, are described. Chapter 16 of this technical report describes the discussion on the containment ultimate pressure capability, in which the ultimate containment capability is evaluated as 216 psia. It is concluded from these evaluations that the containment integrity is sufficiently maintained against the challenge from hydrogen burn associated with 100% cladding-water reactions."

The staff has reviewed this response and has identified that the following needs to be addressed by the applicant:

The staff does not agree with MHI's position that the structural integrity of the PCCV should be evaluated with different criteria than that specified in RG 1.136 for the severe accident case. RG 1.136 section C(5) clearly states that severe accident loads, such as the pressure resulting from an accident that releases hydrogen generated from 100% fuel clad-metal-water reaction plus the pressure resulting from uncontrolled hydrogen burning be considered in the Factored Load Category when evaluating allowable limits from stresses and strains, when using ASME Article CC-3720.

Please provide an American Society of Mechanical Engineers (ASME) Code, Section III, Division 2, Subarticle CC-3720 analysis that demonstrates that containment structural integrity will be maintained in such an event, or please provide an alternate methodology, and clarify the DCD.

The staff has identified this as open item 6.2.5-13."

In their response to this current Question 3.8.1-1, MHI states that they will investigate this problem and incorporate the necessary modifications associated with this Question 3.8.1-1 in the DCD, Revision 2. MHI further states that Chapters 19 and 3 will be revised as necessary to: (1) provide values of  $P_{g1}$  and  $P_{g2}$  (in the RG 1.136 equations); and (2) further clarify the discussion.

For this Question 3.8.1-1, the applicant is requested to demonstrate that the PCCV steel liner does not develop any cracks or tears that could jeopardize the leaktightness function of the liner when the PCCV is subjected to the pressure loads associated with the 100 % metal-water reaction and uncontrolled hydrogen burn. The guidance in RG 1.136 should be considered in determining the factored loads used in any calculations made to provide this demonstration.

---

#### **ANSWER:**

The response to this RAI question was not addressed in DCD Revision 2 and will need to be addressed in a future DCD revision. MHI has received a similar question in the question

06.02.05-36 of RAI 471-3699. To address this issue, MHI will submit a Technical Report in April 2010. Considering the guidance of RG 1.136, the report will demonstrate that the PCCV steel liner does not develop any cracks or tears that could jeopardize the leaktightness function of the liner when the PCCV is subjected to the pressure loads associated with the 100 % metal-water reaction and uncontrolled hydrogen burn, and will be used as a basis for DCD revision to address these issues.

**Impact on DCD**

There is no impact on the DCD.

**Impact on COLA**

There is no impact on the COLA.

**Impact on PRA**

There is no impact on the PRA.

---

---

---

**RESPONSE TO REQUEST FOR ADDITIONAL INFORMATION**

---

---

2/4/2010

**US-APWR Design Certification  
Mitsubishi Heavy Industries  
Docket No. 52-021**

**RAI NO.:** NO. 490-3732 REVISION 0  
**SRP SECTION:** 03.08.01 - Concrete Containment  
**APPLICATION SECTION:** 3.8.1  
**DATE OF RAI ISSUE:** 11/23/2009

---

**QUESTION NO. RAI 03.08.01-3:**

In its response to Question 3.8.1-2, MHI states that the mesh size for the finite element method (FEM) analyses was studied to assure that a sufficiently small mesh size was chosen to accurately determine forces and moments needed for the design of the PCCV. MHI states that convergence is satisfied if the change in calculated forces and moments are observed to be less than +/-10% for those forces and moments controlling the structural design. MHI also states that the mesh size used for the US-APWR is generally smaller than that used for the Japanese APWR.

MHI further states that the mesh size issue was studied using a horizontal load at the top of the cylindrical shell of the PCCV and applying an internal pressure in the PCCV of 10 psig.

The applicant is requested to provide the following information:

The staff finds that the use of +/-10% for the bounds on comparing results from models using progressively smaller (or larger) mesh sizes to be an acceptable criterion. However, the staff notices that in Table 3 and Table 4 in the response that several values for the forces and moments vary by much more than 10%. The applicant is requested to explain why these values with large differences are not important. Also, the data presented in Table 1 in the response that compared mesh size used for the USAPWR with that used for the Japanese pressurized water reactor (PWR) do not provide any supporting information for meeting the convergence criterion. MHI is requested to provide additional information on a convergence study performed for the mesh used in US-APWR.

---

**ANSWER:**

Tables 3, 4, and 5 from the original response to RAI 223-1996 Question 3.8.1-2 have been repeated below for ease of reference, except that the controlling loads are now indicated by note 3 in each table.

In the response to RAI 223-1996 Question 3.8.1-2, Table 3 for the horizontally applied convergence study load identified the force  $N_{tan}$  at the 180 degree azimuth as having a difference greater than 10% due to a change in mesh size. However, the controlling value for the force  $N_{tan}$

actually occurs at the 90 degree azimuth as presented in Table 4. The value for that force is 9.5 times or more greater than the  $N_{tan}$  force at 180° and, as shown in Table 4, does not change more than 10% due to changes in mesh size that were examined in the convergence study. Similarly, Table 4 identified the forces and moments  $N_{\theta}$ ,  $N_{\phi}$ ,  $M_{\theta}$ ,  $M_{\phi}$ , and  $Q_{rad\phi}$  as having differences greater than 10% due to a change in mesh size. However, with respect to selection of mesh size, the controlling values for those forces and moments actually occur either at the 180 degree azimuth for the horizontally applied load as shown in Table 3 or for the internal pressure loading documented in Table 5. As with the  $N_{tan}$  design force, the magnitudes of these forces are very low compared to the design forces. A large percentage change in magnitude is still a very low, inconsequential, force when compared to the controlling force. Therefore, the differences due to changes in mesh size are not important because they are captured by the controlling loads, which have been shown to not change more than 10% due to changes in mesh size.

For Table 5, a change of approximately 12% occurs in  $M_{\theta}$  and  $M_{\phi}$  if the mesh size is doubled in size compared to the design mesh size. However, if the mesh size is decreased by 1/2,  $M_{\theta}$  and  $M_{\phi}$  increase by approximately 5%. This demonstrates that the size of the design mesh is sufficiently fine to capture the controlling moments in the design analyses.

Further, the convergence study represents a general study to determine mesh size used for the overall model of the containment shell. It is not used to determine mesh size in local areas of concern such as at large penetrations like the equipment hatch, main steam penetrations, or personnel airlocks. In these areas the force  $Q_{rad\theta}$ , which is representative of a concentrated punching shear force may be a controlling design force. However, as stated in DCD Subsection 3.8.1.4.1.1, "when considering areas, such as the main steam penetration, concentrated load, or reaction areas, the critical location for shear is generally one-half the thickness away from the opening edge and, the element size should account for this fact." Therefore, although the convergence study identifies that the force  $Q_{rad\theta}$  changes more than 10% due to a change in mesh size, this is acceptable because the purpose of the convergence study is only to validate the mesh size used for the overall model of the containment shell, and not at areas of large penetrations.

Tables 3, 4, and 5 represent a comparison of mesh sizes for the US-APWR to demonstrate that the size of the mesh actually used in the analyses of the PCCV meets the stated convergence criteria that when the mesh size is halved the controlling forces and moments change by less than 10%. Table 1 of the response to previous RAI 223-1996 Question 3.8.1-2 is only a comparison of mesh sizes used in Japan versus the mesh size used for the US-APWR. Table 2 is an inadvertent repeat of the data in Table 1 and can be disregarded.

**Table 3 Comparison of Maximum Force and Moment (Horizontal Load)  
(at around 180°<sup>1</sup> in azimuth angle)  
(Loading Direction: -180°->0° in azimuth angle)**

		$N_{\theta}^3$	$N_{\phi}^3$	$N_{tan}$	$M_{\theta}^3$	$M_{\phi}^3$	$Q_{rad\theta}$	$Q_{rad\phi}^3$
Model1 (Twice)	FEM	1283	6649	363	-5395	-31704	-1	-296
	Ratio <sup>2</sup>	1.00	0.99	2.00	0.91	0.91	1.00	0.97
Model2 (Design)	FEM	1285	6691	182	-5921	-34794	-1	-305
	Ratio <sup>2</sup>	1.00	1.00	1.00	1.00	1.00	1.00	1.00
Model3 (Half)	FEM	1291	6707	91	-6142	-36109	0	-309
	Ratio <sup>2</sup>	1.00	1.00	0.50	1.04	1.04	0.00	1.01

1: 178.5° for Model1, 177° for Model2 and 174° for Model3

2: The ratio to the results of the Model2

3: The components controlling PCCV structural design

**Table 4 Comparison of Maximum Force and Moment (Horizontal Load)  
(at around 90°<sup>1</sup> in azimuth angle)  
(Loading Direction: -180°->0° in azimuth angle)**

		$N_{\theta}$	$N_{\phi}$	$N_{tan}^3$	$M_{\theta}$	$M_{\phi}$	$Q_{rad\theta}$	$Q_{rad\phi}$
Model1 (Twice)	FEM	0	0	3477	0	0	-8	0
	Ratio <sup>2</sup>	-	-	1.00	-	-	0.61	-
Model2 (Design)	FEM	67	351	3466	-310	-1823	-14	-16
	Ratio <sup>2</sup>	1.00	1.00	1.00	1.00	1.00	1.00	1.00
Model3 (Half)	FEM	34	176	3468	-161	-945	-16	-8
	Ratio <sup>2</sup>	0.50	0.50	1.00	0.52	0.52	1.17	0.51

1: 91.5° for Model1, 93° for Model2 and 90° for Model3

2: The ratio to the results of the Model2

3: The components controlling PCCV structural design

**Table 5 - Comparison of Maximum Force and Moment (Internal Pressure)  
(at around 180°<sup>1</sup> in azimuth angle)**

		$N_{\theta}^3$	$N_{\phi}$	$N_{tan}$	$M_{\theta}^3$	$M_{\phi}^3$	$Q_{rad\theta}$	$Q_{rad\phi}^3$
Model1 (Twice)	FEM	9557	0	0	18022	105999	0	1451
	Ratio <sup>2</sup>	1.00	-	-	0.88	0.88	-	0.94
Model2 (Design)	FEM	9578	0	0	20565	120958	0	1540
	Ratio <sup>2</sup>	1.00	-	-	1.00	1.00	-	1.00
Model3 (Half)	FEM	9581	0	0	21686	127550	0	1579
	Ratio <sup>2</sup>	1.00	-	-	1.05	1.05	-	1.03

1: 178.5° for Model1, 177° for Model2 and 174° for Model3

2: The ratio to the results of the Model2

3: The components controlling PCCV structural design

**Impact on DCD**

There is no impact on the DCD.

**Impact on COLA**

There is no impact on the COLA.

**Impact on PRA**

There is no impact on the PRA.

---

---

**RESPONSE TO REQUEST FOR ADDITIONAL INFORMATION**

---

---

2/4/2010

**US-APWR Design Certification  
Mitsubishi Heavy Industries  
Docket No. 52-021**

**RAI NO.:** NO. 490-3732 REVISION 0  
**SRP SECTION:** 03.08.01 - Concrete Containment  
**APPLICATION SECTION:** 3.8.1  
**DATE OF RAI ISSUE:** 11/23/2009

---

**QUESTION NO. RAI 03.08.01-4:**

In its response to Question 3.8.1-3, Part (a) MHI states that by conservatively assuming that the lower bound for Pult is based on initiation of yielding of steel rebars, prestressing tendons, and liner, then "functional failure" (i.e., liner tears) cannot occur since that would require plastic deformation of at least the liner. MHI states that the estimated ultimate pressure capacity of the PCCV is an absolute lower bound and that the actual value (based on structural failure) would be greater.

In their response to Part (b) of Question 3.8.1-3, MHI addresses the magnitude of stresses in the PCCV structure near major penetrations. This is not responsive to the question in which the staff intended to request that the ultimate pressure capacity of the penetration assemblies be determined, not the PCCV shell in the vicinity of the large penetrations. In other words the staff asks in Question 3.8.1-3 for the estimated pressure capacity of the airlock and equipment hatch metal assemblies themselves, not the PCCV shell. Further, MHI states that because additional reinforcement is provided in the PCCV at large major penetrations, these areas are stronger than the PCCV in the free-field (i.e., away from the penetrations.) This does not seem to be self evident, since the strength of the PCCV in the vicinity of the large penetrations depends on the amount and location of the additional reinforcement.

The applicant is requested to provide the following information:

The applicant is requested to provide an evaluation of the ultimate pressure capacity of the steel containment penetration components, specifically the airlock assemblies and the equipment hatch. This evaluation should include an assessment of the leaktightness of gasketed and /or sealed doors used in the airlocks. In addition to the structural integrity calculations, the applicant is requested to explain how leakage from the various containment elements (e.g., penetrations, bolted connections, seals, hatches, bellows) were evaluated and what leakage acceptance criteria were utilized to verify the final ultimate capacity of the containment.

---

**ANSWER:**

MHI has received a similar question in the Follow-up Question to RAI 19-291 of RAI 433-3001. To address this issue, MHI will submit a Technical Report in April 2010, which evaluates the ultimate capacity of the containment, including steel containment penetration components, specifically the airlock assemblies and the equipment hatch. The report will include an assessment of the leaktightness of gasketed and/or sealed doors used in the airlocks. In addition to the structural integrity, the report will address how leakage from the various containment elements (e.g., penetrations, bolted connections, seals, hatches, bellows) was evaluated and what leakage acceptance criteria were utilized to verify the final ultimate capacity of the containment.

Following is a general discussion of the basis/approach and report contents:

The equipment hatch and the personnel airlocks are designed, constructed and installed in accordance with ASME Section III, Division 1 Subsection NE, Class MC Components and must also meet pertinent requirements of RG 1.136.

The equipment hatch and air locks are required to be tested as part of the Prestressed Concrete Containment Vessel which is to be tested for Structural Integrity in accordance with ASME Section III, Division 2 Article CC-6000 using a test pressure of 1.15 times the containment pressure.

The leak tightness is assured by using double gasket seals that can be tested during the plant lifetime and the hatch cover and the personnel airlock doors are to be designed to open inward so that in the event of an accident, the doors are pressure seated and the seals are put in compression by the applied pressure. Typical gaskets have been tested for severe accident conditions as described in NUREG/CR-5096 as well as in NUREG/CR-5118. The gaskets for the US-APWR will be similar to those tested in the NUREG reports. Also, the flanges of the equipment hatch and the personnel airlock doors are stiff enough so that rotation is limited so that the seals remain in compression due to pressures that may exceed the accident pressure.

**Impact on DCD**

There is no impact on the DCD.

**Impact on COLA**

There is no impact on the COLA.

**Impact on PRA**

There is no impact on the PRA.

---

---

---

**RESPONSE TO REQUEST FOR ADDITIONAL INFORMATION**

---

---

2/4/2010

**US-APWR Design Certification  
Mitsubishi Heavy Industries  
Docket No. 52-021**

**RAI NO.:** NO. 490-3732 REVISION 0  
**SRP SECTION:** 03.08.01 - Concrete Containment  
**APPLICATION SECTION:** 3.8.1  
**DATE OF RAI ISSUE:** 11/23/2009

---

**QUESTION NO. RAI 03.08.01-5:**

In its response to Part (a) of Question 3.8.1-5 MHI explains that the soil springs used in the analysis of the PCCV superstructure are elastic springs with tension capability. This is done to simplify the analysis and conservatively maximizes the magnitude of the forces and moments used in the design of the PCCV. MHI states further that the soil springs used in the analysis for design of the R/B-PCCV basemat do not have tension capabilities. MHI states that all spring values for the FE model are determined based on the SSI lumped values given in the DCD (Table 3H.2-14). MHI states that they will modify Subsection 3.8.5.4.3 to clarify that the individual nodal springs of the FE model do not have rotational stiffness.

For Part (b) of the question MHI states that their rationale for the use of different springs used to model the supporting soil is contained in their response to Part (a) above. MHI presents tabulated values of these different springs as requested in the RAI.

For Part (c) of the question the applicant states that they will revise DCD Subsection 3.8.5.4.2 to clarify that the Newmark 100-40-40 method is used to combine the three components of the seismic load. The Newmark method is chosen because it provides more realistic representation of the magnitudes of the resulting compressive and tensile stresses acting on the reinforced concrete cross sections.

For Part (d) of the question MHI explains that what is meant by the term "beyond" in DCD Subsection 3.8.1.4.1.1 is that the results of the analysis using the elastic approach envelope those obtained using an "inelastic" approach. MHI further states that the Square Root of the Sum of the Squares (SRSS) method used for calculating the seismic loads for the structural design of the PCCV is in accordance with the requirements of ASME Code, Article CC-3520 for the shear reinforcement design. For loading other than shear MHI also used SRSS to standardize the overall PCCV design.

For Part (e) of the question MHI explains that in order to fully respond to this part of the question they will need to furnish NRC with "backup data to substantiate their claim that the [stress] redistribution effects are insignificant."

The applicant is requested to provide the following information:

1. For Part (a) of their response, MHI stated that the springs are assigned tension capacity with the intent to simplify the analysis and conservatively maximize the design forces and moments used for the design of the PCCV superstructure. MHI is requested to provide numerical data to substantiate the claim that use of the springs with tension capacity maximizes the design forces and moments for the design of the PCCV superstructure.
2. For Part (b), MHI presents the soil spring constant for each of the three directions per unit area for the FE model in Table 1. These spring constants are the average values over the entire basemat of the dynamic soil springs calculated based on the American Society of Civil Engineers (ASCE) 4-98. The staff finds that MHI's approach is unacceptable because these springs do not reproduce the theoretical distribution of the soil pressure for a uniform displacement of the foundation. Further, MHI is requested to check the units for the vertical spring constant for Method 2,  $k_{v2}$ , mentioned in their response, and provide an explanation for why it does not depend on the angle of rotation. Does  $k_{v2}$  have the tension capability? MHI is also requested to provide the criteria for "lift off" used in the analysis and explain the meaning of "Main loading direction" stated in Table 2 of their response. Are there any minor loading directions? If yes, please describe them. Are vertical soil springs used for any minor loading directions?
3. For Part (c) of MHI's response their explanation of why the Newmark 100-40-40 method is better than the SRSS method for the non-linear analysis is not acceptable because the reason given doesn't seem to have a rational technical basis. These two methods are used to calculate the seismic response due to the excitations of the three components (two horizontal and one vertical component) of the earthquake motion, using the response spectrum method. The underlying assumption for the response spectrum method is linear elastic analysis. So, strictly speaking, both the Newmark 100-40-40 method and the SRSS method should not be used in a non-linear analysis. Therefore, comparing these two methods for a non-linear analysis does not seem to be appropriate. MHI is requested to provide the rationale that clarifies these issues.
4. For Part (d) of the response, MHI states that "the results of the analysis using the elastic approach described in (a) envelope the results of the inelastic approach." This statement may be true by comparing the results obtained by these two methods. However, the staff notices that the assumption and approach used to calculate these results are not theoretically sound for the reasons stated in the evaluation of Part (b) and Part (c) above. The applicant is requested to clarify this statement in view of its response to Parts (b) and (c) above.

For Part (e) the applicant is requested to provide the additional data [mentioned in its response to Part (e) above] that are needed to support the claim that the stress redistribution effects are insignificant.

---

**ANSWER:**

**Part (a)**

The analysis approach that subgrade support springs with tension capacity will maximize the design forces and moments for the PCCV structure will be re-evaluated. A future Technical Report that is currently scheduled to be issued in April 2010 will provide the results of the re-evaluation and any necessary back-up numerical data.

**Part (b)**

The stiffness of soil springs used to model the soil/rock at the base of the R/B mat for the DCD analysis will have non-uniform distribution over the mat area, consistent with the Theory of Elasticity (TE) and experimental observations. Several non-uniform distributions of spring stiffness will be studied, to address the extreme situations resulting from the range of soil/rock stiffness and the range of geo-materials considered in the DCD.

In order to avoid some of the limitations of the Winkler approach that assumes uniform spring stiffness, springs constants will be developed for each finite area (e.g., finite element face) of the basemat as the ratio between contact force acting on that area (i.e., contact pressure times the area) and mat settlement at that location. The proposed approach to address the large range of soil stiffness covered in the DCD is by a numerical (finite element) analysis using ANSYS. The approach further described in the Appendix, will provide the modulus of subgrade reaction,  $k_s$ , at all locations below the mat resting on the surface of an elastic half-space or layer of given thickness and given modulus of deformability. The spring constants will be calculated from  $k_s$  and finite element areas. The soil springs developed following this methodology are based on assumption of a linear elastic material behavior of the soils. However, real soils have a series of distinctive properties listed below that affect the mat settlements and the distribution of contact pressure at the base of the mat:

1. Mat vs. soil/rock stiffness. Mats that are very stiff with respect to the soil have a relatively uniform settlement over the entire area, with varying contact pressures (see Figures 1 and 2 below). Very flexible mats act like loaded surfaces, with approximate uniform distribution of contact pressures and non-uniform settlements. In each case, the resulting spring stiffness will be non-uniformly distributed over the mat surface.
2. Soil type. Coarse grained soils and fine grained soils under drained loading have mostly frictional strength and therefore they are not able to support large contact pressures close to the edges of the mat (the contact pressure is actually zero at the edge for mats at soil surface – see Figure 2b). Rocks and clays under undrained loading conditions have mostly cohesive strength and will support relatively large contact pressures close to mat boundaries, with pressure distributions closer to those obtained from the TE.
3. Nonlinear behavior. At very small strains, soils and rocks behave approximately elastically. The stress-strain relation becomes non-linear at larger strains, and the contact pressures are limited by the soil strength.
4. Dependence of soil moduli on effective stress. It is known that soil deformation moduli increase with effective confining stress leading to larger contact pressures in the central area (see Figure 2b).

The development of the soil springs stiffness will address the aspects discussed above as follows:

1. Mat vs. soil/rock stiffness. A range of soil/rock materials with a wide range of deformation moduli is considered in the DCD, from the lower range of medium dense sands (shear wave velocity  $V_s = 1000$  fps and deformation moduli two orders of magnitude less than concrete) to competent rocks ( $V_s = 8000$  fps and deformation moduli of the same order of magnitude as concrete). There are analytical solutions for the two bounding cases that will be used to benchmark the finite element solutions and to establish necessary modifications of TE solutions to model real soil behavior as follows:
  - A) Soil with  $V_s = 1000$  fps. Rigid mat will be assumed, with uniform settlement over the mat surface and non-uniform contact pressure. Soils with purely cohesive strength will be considered, as explained in point 2 below. The contact pressures

will be calculated by a method based on the TE, with edge values limited by the soil cohesive strength (see Zeevaert 1972). The method is briefly presented below in the Appendix.

- B) Rock with  $V_s = 8000$  fps. Perfectly flexible mat will be assumed, with uniform contact pressures and non-uniform settlements. The settlements will be calculated using the TE and a method described by Bowles (1996) and briefly presented in the Appendix.
2. Soil type. In the case of soils with frictional strength (sands and gravels) the maximum shear strength on a given plane is proportional with the effective stress acting normal to that plane. For loaded areas placed at soil surface, the effective normal stress in any direction is zero immediately near the edge of the mat, and therefore the shear strength at mat edges is zero. For real foundations, placed at a certain depth, the strength of soil below edge (and therefore the contact pressures) is larger than zero but still increases toward the center of the foundation. Intact rocks, on the other hand, have mostly cohesive strength that theoretically does not depend on the applied effective stress. This large range of shear strengths of frictional materials cannot be handled by the TE and can only be addressed numerically using advanced constitutive models. It is proposed, therefore, that only cohesive type materials be considered when calculating soil spring stiffness.
  3. Nonlinear behavior. Given the very large size of the R/B mat, the strain level is within elastic limits for most of the area, except at the edges where shear strains will exceed the elastic limits. This effect will be accounted for by limiting soil strength as described at point 1A above. Therefore there is no need to consider soil non-linearity in addition to limiting the edge contact pressures to soil strength.
  4. Dependence of soil moduli on effective stress. This phenomenon leads to increase in soil stiffness toward the center of the mat and, for the structural configuration analyzed here, it is likely to induce lower stresses in the mat. A final check will be performed by finite element analysis using a hyperelastic model for soil (e.g., the neo-Hookean model implemented in ANSYS) that accounts for change in stiffness as a function of effective confining stress. If the change in soil stiffness distribution is significant and leads to larger stresses in the mat, it will be implemented in calculating spring stiffness.

The standard design will use stiffness and distribution of soil spring that will be obtained considering the two bounding cases of mat vs. soil stiffness and several cases in between. The mat will be designed to withstand the envelope of bending moments and shear forces obtained from the different foundation analyses.

#### **References for Item 2**

Bowles, J.E, Foundation Analysis and Design, 5th edition, McGraw-Hill, 1996.

Terzaghi, K. & Peck, R.B, Soil Mechanics in Engineering Practice, 2nd edition, Wiley, 1968.

Zeevaert, L., Foundation Engineering for Difficult Subsoil Conditions, Van Nostrand Reinhold, 1972.

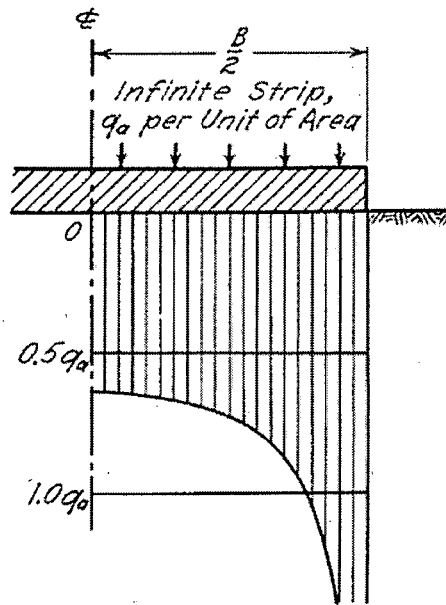


Fig. 42.1. Distribution of contact pressure on base of uniformly loaded rigid footing of very great length, resting on perfectly elastic, homogeneous, and isotropic subgrade.

Figure 1 After Terzaghi & Peck (1968).

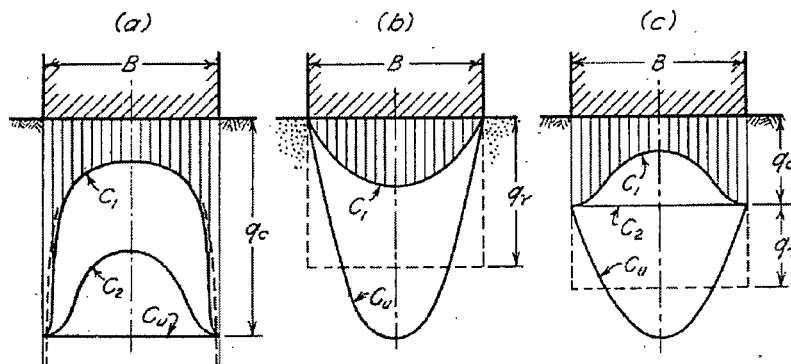


Fig. 42.2. Distribution of contact pressure on base of smooth rigid footing supported by (a) real, elastic material; (b) cohesionless sand; (c) soil having intermediate characteristics. Curves  $C_u$  refer to contact pressure when footing is loaded to ultimate value.

Figure 2 Pressure Distribution at (b) corresponds to a relatively narrow footing (after Terzaghi & Peck, 1968). The shear strength of soil is denoted as:  $q_c$  (cohesive) and  $q_f$  (frictional).

## APPENDIX for Answers to Question 03.08.01-5 – Part (b)

### A1. ANSYS Analysis

An example is presented on estimating the modulus of subgrade reaction ( $k_s$ ) for a R/B mat supported by a soil with shear wave velocity  $V_s = 2500$  fps represented as an elastic halfspace, is presented in figures A1 thru A4. The analysis is performed for one quarter of the pad to take advantage of symmetry. The extension of the analysis domain in horizontal direction has to ensure negligible displacements and changes in stress at the lateral boundaries. A domain about 3x larger than the pad in both directions is sufficient to reduce these errors below 5%. The vertical extension is either to a practically non-deformable layer (with respect to the soil below the mat) or to about 3 times the width of the foundation for a half-space.

The mat is represented by thick shell (SHELL43) elements and the soil by 3D structural solid (SOLID45) elements. A no-slip interface is assumed to simplify the calculations. Figure A1 shows the deformed mesh due to a uniform pressure of 10 ksf. The results of interest are the mat settlements (represented by contours in Figure A2) and the vertical stresses in soil immediately below the mat (contours in Figure A3). The modulus of subgrade reaction at each location below the mat is obtained by dividing settlements by vertical stresses (contours in Figure A4).

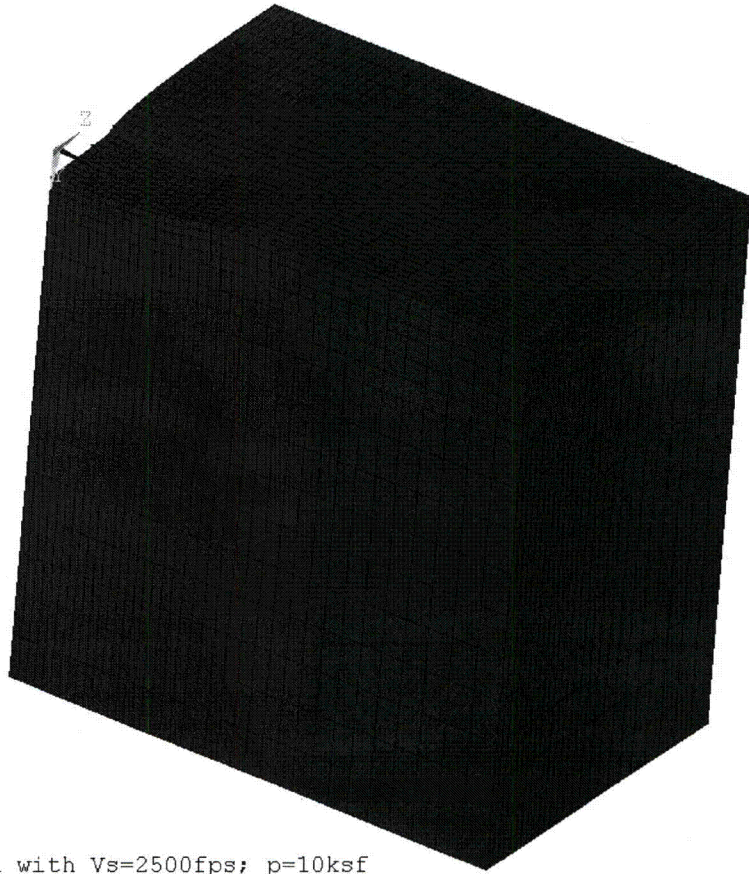
### A2. Infinitely Rigid Mat

The contact stresses can be obtained assuming uniform settlements over the entire mat and using TE equations. The resulting stresses at the edges of the mat are theoretically infinite. Zeevaert (1972) presents a relatively simple method to reduce the stresses at the edges of the mat to some limit values calculated based on soil shear strength, and redistribute the remaining pressures over the mat area. The method is presented in Figure A5 for a strip foundation. This method will be extended for rectangular foundations.

### A3. Very Flexible Mat

In the case of flexible mat, its stiffness can be neglected and the contact stresses are taken equal to the uniform pressure applied on the mat and denoted by  $q_0$  as shown in Figure A6. The settlements below the corner of a rectangular loaded area on an elastic half-space are calculated using TE equations – method presented by Bowles (1996) as illustrated in Figure A6. For each location, the mat is divided into four rectangles with a common corner at that location, and the settlements  $\Delta H_i$ ,  $i=1, \dots, 4$ , produced by each rectangle,  $i$ , are calculated using equation (5-16) in Bowles (1996) – shown in Figure A6. The modulus of subgrade reaction at each location is calculated as:  $k_s = q_0 / \sum \Delta H_i$ .

1  
DISPLACEMENT  
STEP=1  
SUB =1  
TIME=1  
DMX =.145179



RB Mat on Soil with  $V_s=2500\text{fps}$ ;  $p=10\text{ksf}$

**Figure A1** Finite Element Mesh and Deformed Shape for Analysis of a 30ft Thick Concrete Mat (modeled by shell finite elements and not shown here) loaded by uniform pressure,  $p = 10\text{ksf}$ , and supported by soil with shear wave velocity of 2500fps assumed elastic.



**Figure A2** Contours of Computed Mat Settlements – in ft (one quarter of the mat is shown, the center of mat is in the lower left corner of the figure)

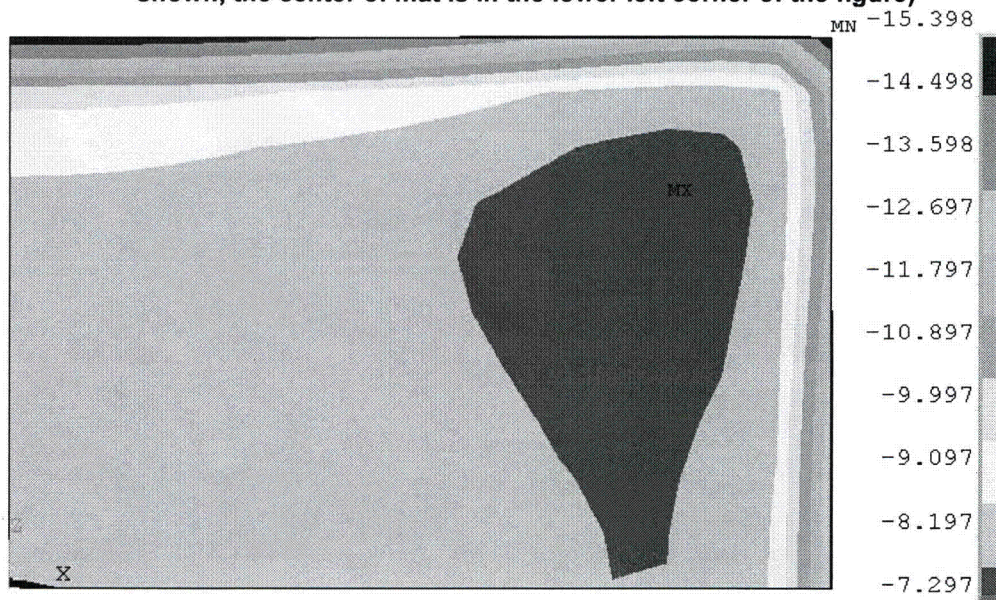


**Figure A3.** Contours of Computed Vertical Stresses in Soil, Below Mat – in ksf (one quarter of the mat is shown, the center of mat is in the lower left corner of the figure)

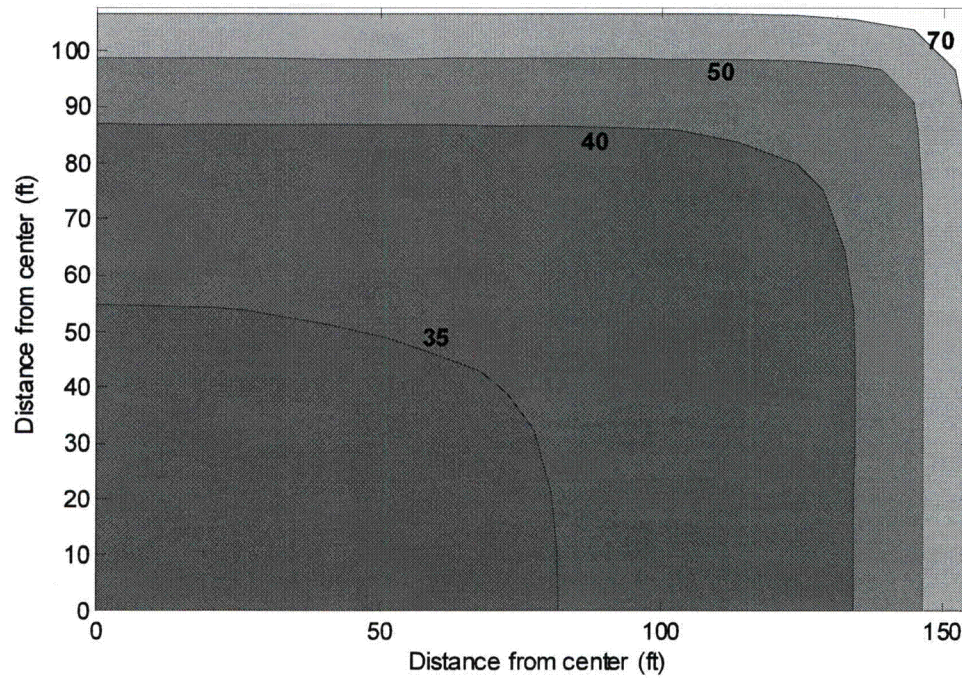


**Figure A4** Contours of Modulus of Subgrade Reaction (pci) Below a 30ft Thick, 215ft by 310ft Rectangular Concrete Mat, loaded by uniform pressure and supported by elastic soil with shear wave velocity of 2500fps. Only one quarter of the mat is shown (layout described in Figure A1).

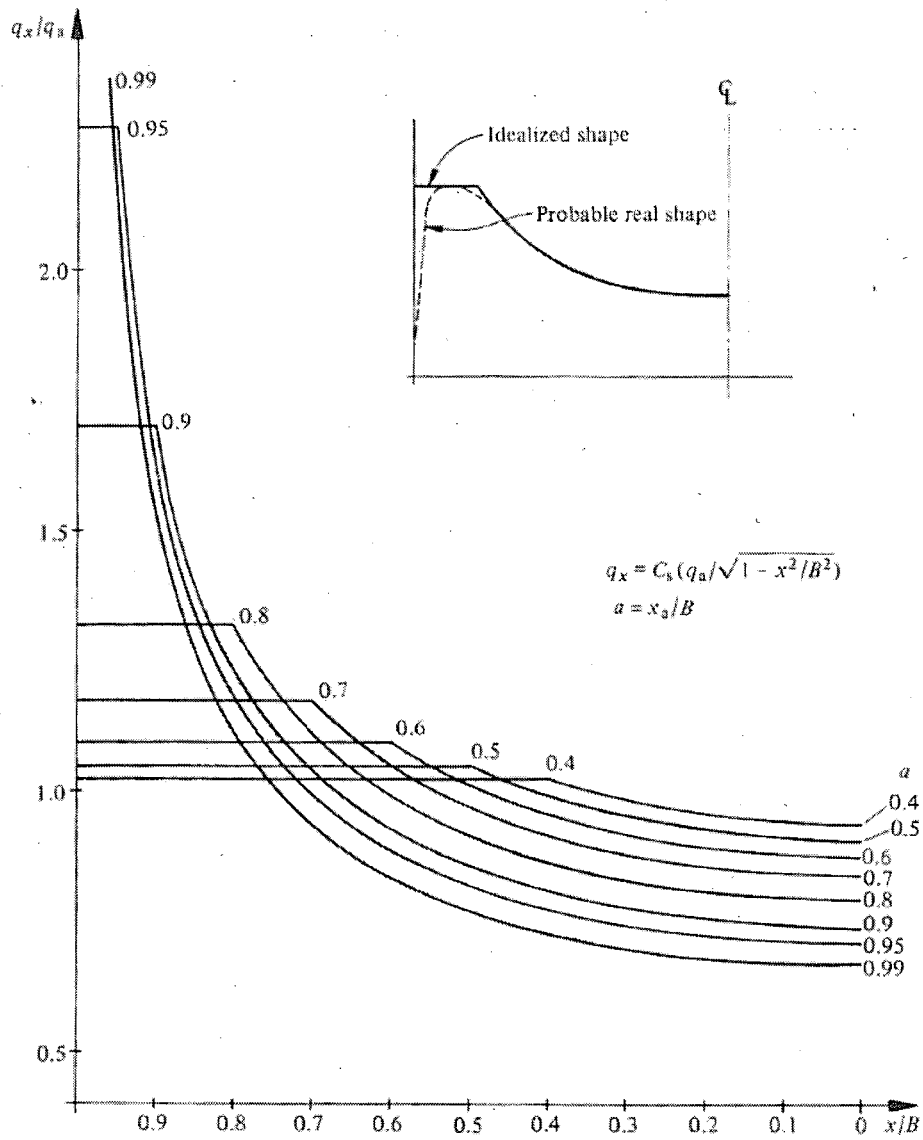


**Figure A5** Contact Pressure Distribution Under a Rigid Strip Foundation on Elastic-Plastic Soil, for Various Values of the Limiting Pressure Governed by Soil Shear Strength (after Zeevaert, 1972).

## IMMEDIATE SETTLEMENT COMPUTATIONS

The settlement of the corner of a rectangular base of dimensions  $B' \times L'$  on the surface of an elastic half-space can be computed from an equation from the Theory of Elasticity [e.g., Timoshenko and Goodier (1951)] as follows:

$$\Delta H = q_0 B' \frac{1 - \mu^2}{E_s} \left( I_1 + \frac{1 - 2\mu}{1 - \mu} I_2 \right) I_F \quad (5-16)$$

where  $q_0$  = intensity of contact pressure in units of  $E_s$   
 $B'$  = least lateral dimension of contributing base area in units of  $\Delta H$   
 $I_1$  = influence factors, which depend on  $L'/B'$ , thickness of stratum  $H$ , Poisson's ratio  $\mu$ , and base embedment depth  $D$   
 $E_s, \mu$  = elastic soil parameters—see Tables 2-7, 2-8, and 5-6

The influence factors (see Fig. 5-7 for identification of terms)  $I_1$  and  $I_2$  can be computed using equations given by Steinbrenner (1934) as follows:

$$I_1 = \frac{1}{\pi} \left[ M \ln \frac{(1 + \sqrt{M^2 + 1}) \sqrt{M^2 + N^2}}{M(1 + \sqrt{M^2 + N^2 + 1})} + \ln \frac{(M + \sqrt{M^2 + 1}) \sqrt{1 + N^2}}{M + \sqrt{M^2 + N^2 + 1}} \right] \quad (a)$$

$$I_2 = \frac{N}{2\pi} \tan^{-1} \left( \frac{M}{N \sqrt{M^2 + N^2 + 1}} \right) \quad (\tan^{-1} \text{ in radians}) \quad (b)$$

where  $M = \frac{L'}{B'}$        $N = \frac{H}{B'}$   
 $B' = \frac{B}{2}$  for center; =  $B$  for corner  $I_1$   
 $L' = L/2$  for center; =  $L$  for corner  $I_1$

**Figure A6** Method Based on the Theory of Elasticity for Computing the Settlement,  $\Delta H$ , below the corner of a rectangular, perfectly flexible foundation, loaded by a uniform pressure,  $q_0$ , and supported by an elastic soil layer with Young's modulus  $E_s$  (excerpt from Bowles 1996).

### **Part (c)**

As explained above in the discussion of Item 2, the foundation design is based on the results of analyses where the soil subgrade stiffness is modeled using linear elastic constitutive behavior. As previously clarified in the response to Question 3.8.1-5(a) of the RAI 223-1996, the term "non-linear" was used to refer to the use of springs with compression capacity only for purposes of the R/B foundation analyses. This is a traditional and conventional approach for foundation analyses, particularly for cases where partial uplift may occur. In this sense, the analyses performed are not non-linear. Therefore the use of the 100-40-40 combination method is deemed acceptable for directional combination. Further to the previous explanation provided in response to RAI 223-1996 Question 3.8.1-5(c): In accordance with ASCE 4-1998, Commentary Section C3.2.7.1.2, "the 100-40-40-Percent Rule is based on the observation that the maximum increase in the resultant for two orthogonal forces occurs when these forces are equal. The maximum value is 1.4 times one component. The 100-40-40-Percent Rule is deemed a reasonable procedure to use given the basic uncertainties involved."

The expression "inelastic" which is used in Subsection 3.8.1.4.1.1 for describing soil springs will be removed and additional clarification will be provided, subsequent to the completion of the Technical Report described in Part (a) above.

### **Part (d)**

This item will be addressed in a future Technical Report as discussed in Part (a) above.

### **Part (e)**

The analysis approach that subgrade support springs with tension capacity will maximize the design forces and moments for the PCCV structure will be re-evaluated as stated in Part (a) above. The re-evaluation will investigate whether use of springs with tension capacity results in maximized design forces and moments for the PCCV structure. If confirmed as valid, then associated data which address redistribution effects will be included in the Technical Report as described in Part (a).

#### **Impact on DCD**

There is no impact on the DCD.

#### **Impact on COLA**

There is no impact on the COLA.

#### **Impact on PRA**

There is no impact on the PRA.

---

---

---

**RESPONSE TO REQUEST FOR ADDITIONAL INFORMATION**

---

---

2/4/2010

**US-APWR Design Certification  
Mitsubishi Heavy Industries  
Docket No. 52-021**

**RAI NO.:** NO. 490-3732 REVISION 0  
**SRP SECTION:** 03.08.01 - Concrete Containment  
**APPLICATION SECTION:** 3.8.1  
**DATE OF RAI ISSUE:** 11/23/2009

---

**QUESTION NO. RAI 03.08.01-6:**

In its response to Question 3.8.1-2, Part (a) of the question, MHI states that the PCCV buttresses are modeled using shell elements as part of the PCCV in the 3-D global FEM model. A figure is included that shows an enlargement of this detail. MHI provides an explanation of how the primary and secondary forces are considered in the design, citing the ASME Code, Table CC-3136.6-1. The explanation includes a discussion of secondary forces due to creep shrinkage and thermal input forces. MHI describes the use of a post-processor to evaluate the results of the FE model analysis.

For Part (b) of the question MHI states that the discontinuity effects of the buttresses are captured by the fact that the centerlines of the buttress shell elements and the wall shell elements are offset from each other. It is stated that the detailed design of the tendon end anchorage reinforcement also considers local effects. MHI points out that the design of the tendon and tendon anchorage details needs to be confirmed by the COL applicant based on as-built material properties of the tendon system and the concrete.

In general, MHI's response is reasonable and acceptable to the staff. However, in Part (b) of the MHI's response, MHI states that "The thickness of the buttress shell elements is 92" which is 40" thicker than the cylindrical wall elements. The centerlines of the buttress elements are accordingly offset from the centerlines of the wall elements. Therefore, the discontinuity effects of the buttresses are captured automatically by the global FE model analyses." The staff notices that MHI used the computer code ANSYS Release 11 (DCD Reference 3.8-14) to check the NASTRAN results.

The staff is aware that ANSYS (Release 11) will not automatically account for the discontinuity effects due to the offset of the centerlines. Therefore, MHI is requested to provide information that shows how discontinuity effects are captured automatically in the ANSYS analysis.

---

**ANSWER:**

The thickness of the buttress shell elements is 92" and the typical PCCV shell thickness is 52". This results in a 48" offset in thickness between the buttress and the external surface of the

PCCV cylinder wall. See Figure 1 below. This offset results in a difference in centerline position of  $100''/2 - 52''/2 = 24''$ . The previous NASTRAN 3-D FE model performs stress analysis of the cylindrical wall and buttresses using shell elements at the location of the wall center with offset defining function of NASTRAN itself for buttresses. Therefore, in the case of NASTRAN, the offset effects of the buttresses are captured automatically by the global FE model analyses.

In accordance with ASME Code Section CC-3320, "shell analysis may be based on membrane theory, additional consideration is required for bending and shear forces at penetrations, intersection with base mat, discontinuities, and the stresses and strains caused by temperature variations." A model constructed using shell elements is considered to be an acceptable technique and is appropriate to the geometry of the PCCV containment.

In order for the ANSYS analysis model to account for the discontinuity effect, plate elements which reflect a more realistic geometry and thickness will be placed at the centerline of the buttress. The shell elements with variable thickness at nodes will be used to represent the continuity of the wall to the buttress. Forces and moments will be applied to the centerline of the elements to represent the post-tensioning forces on the tendons.

The structural design of the PCCV at the locations of the buttresses and regions away from discontinuities (buttress) are evaluated for radial and membrane shear in accordance with CC-3421.4 and Table CC-3136.6-1 of the ASME Code. Tendon end anchor reinforcement is provided to control cracking in the end anchor zone as required by Section CC-3543.

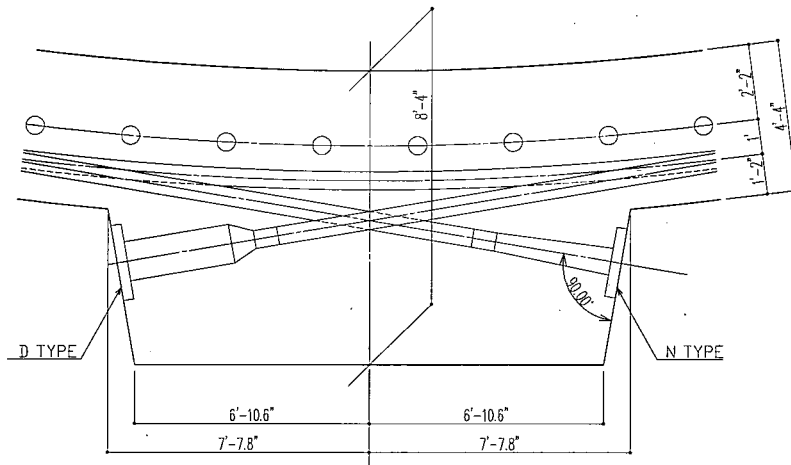


**Figure 1 Plan Detail of Typical Buttress**

**Impact on DCD**

There is no impact on the DCD.

**Impact on COLA**

There is no impact on the COLA.

**Impact on PRA**

There is no impact on the PRA.

---

---

**RESPONSE TO REQUEST FOR ADDITIONAL INFORMATION**

---

---

2/4/2010

**US-APWR Design Certification  
Mitsubishi Heavy Industries  
Docket No. 52-021**

**RAI NO.:** NO. 490-3732 REVISION 0  
**SRP SECTION:** 03.08.01 - Concrete Containment  
**APPLICATION SECTION:** 3.8.1  
**DATE OF RAI ISSUE:** 11/23/2009

---

**QUESTION NO. RAI 03.08.01-7:**

In its response to Part (a) of Question 3.8.1-7, MHI states that the average and equivalent linear gradients are the components of the equivalent linear temperature distribution that is applied to the FE model for the purposes of structural design. Formulas are presented by MHI for the average and equivalent linear gradients of the temperature in the sections of the PCCV, along with sketches used to illustrate these formulations.

In response to Part (b) of the question MHI explains that the thermal gradients across the PCCV cylindrical walls, basemat, and dome are calculated from the formulas described in (a) above. MHI notes that they include the effects of the liner plate on these temperature distributions. The results of these calculations are presented in several tables in the response which include the results for both summer and winter conditions. Several figures are presented that show graphically the temperature distributions in the PCCV dome, cylindrical walls, and the basemat.

The staff finds that MHI presents an acceptable explanation of the terms "average" and equivalent linear gradients" that provides an adequate clarification of these terms. In addition, the response includes detailed information on the formulas used in these temperature calculations. The applicant presents several pages of figures that show the temperature distributions in the PCCV cylindrical walls and dome, and for the PCCV basemat.

The applicant is requested to provide the following information:

MHI points out that the methodology used to calculate these temperature distributions is almost the same as that of American Concrete Institute (ACI)-349, except that MHI also considers the effect of the steel liner on these temperature distributions. The applicant is requested to explain the significance of including the ¼ in. steel liner plate in the heat transfer calculations (as opposed to the approach used in ACI 349).

---

**ANSWER:**

Including the effect of the ¼ in. steel liner plate in the calculations for the average temperature and the equivalent linear gradient across the PCCV cylinder wall and dome produces more

conservative stress distributions in the design of the PCCV structure. Comparison of the calculated average temperatures and the equivalent linear gradients, with and without considering the ¼ in. steel liner plate, are shown in Tables 1(1) and 1(2) below for the Normal Operating and LOCA conditions, respectively.

The governing equivalent linear gradients which control the PCCV structural design are from a LOCA condition during winter with the outside of the PCCV exposed to open air. Considering the steel liner plate is shown in Table 1(2) to increase the equivalent linear gradient from 16% to 36% above the condition when it is not considered, and is therefore appropriate for the PCCV structural design.

**Table 1(1) Average Temperature and Equivalent Linear Gradient (Normal Operating)**

	Region	Out Side Condition of CV	Td: Average Temperature (°F)			ΔTg/t: Linear Gradients of Temperature/Thickness (°F/in.)		
			w/Liner	wo/Liner	w/wo	w/Liner	wo/Liner	w/wo
Winter	Dome	Open Air	37	34	1.09	3.11	2.65	1.17
	Cylinder	Open Air	37	34	1.09	2.65	2.31	1.15
		Room	80	77	1.04	1.25	0.90	1.39
Summer	Dome	Open Air	122	118	1.03	0.67	0.09	7.44
	Cylinder	Open Air	121	118	1.03	0.49	0.08	6.13
		Room	116	112	1.04	0.65	0.25	2.60

**Table 1(2) Average Temperature and Equivalent Linear Gradient (LOCA)**

	Region	Out Side Condition of CV	Td: Average Temperature (°F)			ΔTg/t: Linear Gradients of Temperature/Thickness (°F/in.)		
			w/Liner	wo/Liner	w/wo	w/Liner	wo/Liner	w/wo
1 hour after LOCA								
Winter	Dome	Open Air	57	46	1.24	5.58	4.11	1.36
	Cylinder	Open Air	53	44	1.20	4.42	3.37	1.31
		Room	96	87	1.10	2.96	1.93	1.53
Summer	Dome	Open Air	139	128	1.09	2.83	1.39	2.04
	Cylinder	Open Air	135	127	1.06	2.05	1.02	2.01
		Room	130	122	1.07	2.22	1.19	1.87
24 hours after LOCA								
Winter	Dome	Open Air	100	89	1.12	8.65	7.17	1.21
	Cylinder	Open Air	89	80	1.11	6.90	5.85	1.18
		Room	131	122	1.07	5.38	4.33	1.24
Summer	Dome	Open Air	176	166	1.06	5.53	4.07	1.36
	Cylinder	Open Air	167	159	1.05	4.26	3.21	1.33
		Room	162	154	1.05	4.43	3.39	1.31
4 days after LOCA								
Winter	Dome	Open Air	112	104	1.08	6.80	5.67	1.20
	Cylinder	Open Air	102	96	1.06	5.76	4.95	1.16
		Room	143	136	1.05	4.24	3.43	1.24
Summer	Dome	Open Air	184	176	1.05	3.65	2.54	1.44
	Cylinder	Open Air	176	169	1.04	3.05	2.25	1.36
		Room	171	164	1.04	3.24	2.44	1.33
30 days after LOCA								
Winter	Dome	Open Air	96	89	1.08	5.54	4.61	1.20
	Cylinder	Open Air	93	88	1.06	4.64	3.97	1.17
		Room	132	126	1.05	3.15	2.49	1.27
Summer	Dome	Open Air	164	158	1.04	2.43	1.51	1.61
	Cylinder	Open Air	163	157	1.04	1.96	1.31	1.50
		Room	157	152	1.03	2.17	1.52	1.43

**Impact on DCD**

There is no impact on the DCD.

**Impact on COLA**

There is no impact on the COLA.

**Impact on PRA**

There is no impact on the PRA.

---

---

**RESPONSE TO REQUEST FOR ADDITIONAL INFORMATION**

---

---

2/4/2010

**US-APWR Design Certification  
Mitsubishi Heavy Industries  
Docket No. 52-021**

**RAI NO.:** NO. 490-3732 REVISION 0  
**SRP SECTION:** 03.08.01 - Concrete Containment  
**APPLICATION SECTION:** 3.8.1  
**DATE OF RAI ISSUE:** 11/23/2009

---

**QUESTION NO. RAI 03.08.01-8:**

In its response to Question 3.8.1-8, MHI states that an analysis of the PCCV for seismic loadings determined that the resulting shear forces and moments do not cause cracking at the base of the PCCV cylindrical wall. Based on this MHI concludes that concrete cracking has only an insignificant effect on the natural frequencies of the PCCV. In addition, MHI states that investigation of load combinations of ASME Table CC-3230-1 was also conducted and they concluded that the effects of concrete cracking were not extensive enough to significantly affect these natural frequencies. MHI further states that the results of these analyses (which were omitted from the DCD) could be included if converted to ASME code checks.

The applicant is requested to provide the following information:

1. The staff finds MHI's response not acceptable because the concrete cracking may be caused by other loadings, such as the thermal load. The concrete may be already cracked before the SSE event. The applicant is requested to provide the rationale to support the argument that this scenario is not possible.

Also, in the 6th line of MHI's response it states: "...that cracking was not extensive enough to significantly affect the natural frequencies of the PCCV." This terminology is qualitative and the applicant is requested to provide the actual values that describe the extent of concrete cracking, such as providing a map of concrete cracking of the PCCV. In addition, the applicant is requested to explain the meaning of the second paragraph in the response, including what "results" are referred to in the sentence, and why and how would these results be "converted to ASME Code checks."

---

**ANSWER:**

As previously stated in the response to RAI 223-1996 Question 3.8.1-08, the evaluation of the PCCV stresses under SSE conditions determined that the resulting shear forces and moments do not cause significant cracking of the PCCV, and do not cause cracking at the base of the PCCV cylinder. The previous stress analyses of the PCCV show that besides small localized areas, the pre-stressed concrete of the PCCV remains generally in compression under mechanical loads.

Further, the overall behavior of the PCCV cylinder and dome walls in resisting lateral loads is that of a membrane which is not sensitive to reductions in bending stiffness. Cracking of the PCCV does not occur under normal operating thermal loads but does occur due to accidental thermal loading. SSE, accident pressure, and accident thermal loads are considered concurrently as required by Table CC-3230-1 of ASME Section III. Due to the period of time needed for the accident thermal stresses to develop to the point where there is a potential for cracking, the analyses do not consider maximum SSE and maximum pressure loads to act concurrently with maximum thermal loads. This is permitted by ASME Section III CC-3230(c), which states that the "maximum effects of Pa, Ta, Ra, Rr, and G shall be combined unless a time-history analysis is performed to justify the lower combined values." After return from abnormal thermal load conditions, the initial reduction of stiffness due to any cracking caused by accidental thermal loads will be mostly recovered by the prestress forces.

The US-APWR DCD seismic analyses consider an envelope of responses obtained from analyses of wide range of subgrade conditions. Therefore, the seismic analysis is based on uncracked properties of the prestress concrete since the effect of the possible shift of fundamental frequency of the PCCV due to concrete cracking will be enveloped by the wide range of different subgrade conditions considered.

The effects of concrete cracking on seismic response of the R/B complex will be addressed in detail in a future Technical Report summarizing seismic analysis and effects and extent of cracking, which MHI intends to issue in May 2010.

In the response to the question above regarding the "results", the results of the stress evaluations against applicable ASME Code allowables given in ASME Section III Articles CC-3400 and CC-500 will be included in the Technical Report.

**Impact on DCD**

There is no impact on the DCD.

**Impact on COLA**

There is no impact on the COLA.

**Impact on PRA**

There is no impact on the PRA.

---

---

---

**RESPONSE TO REQUEST FOR ADDITIONAL INFORMATION**

---

---

2/4/2010

**US-APWR Design Certification  
Mitsubishi Heavy Industries  
Docket No. 52-021**

**RAI NO.:** NO. 490-3732 REVISION 0  
**SRP SECTION:** 03.08.01 - Concrete Containment  
**APPLICATION SECTION:** 3.8.1  
**DATE OF RAI ISSUE:** 11/23/2009

---

**QUESTION NO. RAI 03.08.01-9:**

In its response for Part (a) of Question 3.8.1-9, MHI states that thermal forces and moments are reduced according to the concrete cracking depth during the post-processing of the global FE model analysis results. The reduction is based on redistribution of section forces and moments that occurs from the concrete cracking.

For Part (b) of the question MHI explains that the depth of concrete cracking is calculated by determining the neutral axis of the cross-section of the member, along with consideration of strain compatibility among the concrete, liner, tendons, and steel reinforcement. A summary description of the stress verification methodology is presented in this response, including simplified examples to demonstrate the methodology.

The staff finds that MHI's response does not clearly indicate how thermal forces and moments are reduced according to the concrete cracking depth. In MHI's response, a notation,  $\sigma_1$ , is used to denote the extreme fiber stress of the concrete; however, in the example given at the end, an additional notation,  $\sigma_2$ , is introduced without any explanation. MHI is requested to clarify this confusion. Also, MHI is requested to provide a calculation example that is taken from the US-APWR design, and that will have numerical results clearly showing the amount of reduction in forces and moments and the concrete cracking depth.

---

**ANSWER:**

Treatment of thermal forces and moments and further explanation of how they are reduced according to concrete cracking depth, including calculation examples taken from the US-APWR design, will be addressed in a future Technical Report that MHI intends to issue in April 2010.

**Impact on DCD**

There is no impact on the DCD.

**Impact on COLA**

There is no impact on the COLA.

**Impact on PRA**

There is no impact on the PRA.

---

---

---

**RESPONSE TO REQUEST FOR ADDITIONAL INFORMATION**

---

---

2/4/2010

**US-APWR Design Certification  
Mitsubishi Heavy Industries  
Docket No. 52-021**

**RAI NO.:** NO. 490-3732 REVISION 0  
**SRP SECTION:** 03.08.01 - Concrete Containment  
**APPLICATION SECTION:** 3.8.1  
**DATE OF RAI ISSUE:** 11/23/2009

---

**QUESTION NO. RAI 03.08.01-10:**

In its response to Question 3.8.1-10, MHI states that considerations of concrete cracking effects on the global model of the PCCV are discussed in their response to Question 3.8.1-(0)8. It is further stated that the presence and the extent of the cracking within a section, and the distribution of forces and moments within a cracked section, is determined and evaluated as part of the post-processing of the global FE model results.

The staff finds that MHI's response to this question is not acceptable. MHI's response to this question is based on the response to Question 3.8.1-8 in which MHI states that the concrete will not crack. This implies that the redistribution of section forces and moments due to concrete cracking was not included in the analysis. However, the implication in the above response to this Question 3.8.1-10 seems to be that there is cracking and that cracking is determined in the post-processing of the global FE model results. The applicant is requested to explain whether or not concrete cracking was considered in the PCCV analysis. If it was considered, how was it accounted for in the analysis, and how were the forces and moments redistributed?

---

**ANSWER:**

As stated in the response to Questions 3.8.1-08 and 3.8.1-09, this issue will be addressed in detail in a future Technical Report summarizing seismic analysis and effects and extent of cracking, which MHI intends to issue in April 2010.

As previously stated in the response to RAI 223-1996 Question 3.8.1-08, no cracking occurs at the base of the PCCV under SSE conditions and cracking that occurs elsewhere is insignificant with respect to the seismic response.

The seismic analysis methods for the PCCV consider un-cracked concrete properties, and the stiffness of the concrete is not reduced. The analyses of the PCCV show that besides small localized areas, the pre-stressed concrete of the PCCV remains generally in compression under mechanical loads. Cracking of the PCCV does not occur under normal operating thermal loads but does occur due to accidental thermal loading. SSE, accident pressure, and accident thermal loads are considered concurrently as required by Table CC-3230-1 of ASME Section III. Due to

the period of time needed for the accident thermal stresses to develop to the point where there is a potential for cracking, the analyses do not consider maximum SSE and maximum pressure loads to act concurrently with maximum thermal loads. This is permitted by ASME Section III CC-3230(c), which states that the "maximum effects of Pa, Ta, Ra, Rr, and G shall be combined unless a time-history analysis is performed to justify the lower combined values."

Redistribution of forces and moments due to thermal cracking under accident conditions is considered as part of the thermal analyses and will be addressed in the Technical Report. The presence and extent of cracking within a section, and the distribution of forces and moments within a cracked section, are evaluated as part of the post-processing of the global FE model results, as stated in the response to Question 3.8.1-10 of RAI 223-1996. As described in Subsection 3.8.1.4.4 of the DCD, the post-processing methodology accounts for concrete cracking and strain compatibility among concrete, liner, tendons, and reinforcing steel for primary and secondary loads.

**Impact on DCD**

There is no impact on the DCD.

**Impact on COLA**

There is no impact on the COLA.

**Impact on PRA**

There is no impact on the PRA.

---

This completes MHI's responses to the NRC's questions.